Numer Algor (2017) 76:1039–1070
DOI 10.1007/s11075-017-0296-y

ORIGINAL PAPER

A novel cognitive transformation algorithm based on Gaussian cloud model and its application in image segmentation

Chang-Lin Xu[1] **· Guo-Yin Wang**[2]

Received: 1 May 2016 / Accepted: 19 February 2017 / Published online: 27 February 2017

Abstract The representation and processing of uncertain concepts are key issue for both the study of artificial intelligence with uncertainty and human knowledge processing. The intension and extension of a concept can be transformed automatically in the human cognition process, while it is difficult for computers. A Gaussian cloud model (GCM) is used to realize the cognitive transformation between intension and extension of a concept through computer algorithms, including forward Gaussian cloud transformation (FGCT) algorithms and backward Gaussian cloud transformation (BGCT) algorithms. A FGCT algorithm can transform a concept's intension into extension, and a BGCT algorithm can implement the cognitive transformation from a concept's extension to intension. In this paper, the authors perform a thorough analysis on the existing BGCT algorithms firstly, and find that these BGCT algorithms have some drawbacks. They cannot obtain the stable intension of a concept sometimes. For this reason, a new backward Gaussian cloud cognitive transformation algorithm based on sample division is proposed. The effectiveness and convergence of the proposed method is analyzed in detail, and some comparison experiments on

This paper is an expanded version of "G.Y. Wang, C.L. Xu, et al. A Multi-step backward cloud generator algorithm. 8th International Conference, RSCTC2012, Berlin: Springer, 2012, 313-322".

✉ Chang-Lin Xu
xuchlin@163.com

[1] School of Mathematics and Information Science, Beifang University of Nationalities, Yinchuan, China

[2] Institute of Electronic Information Technology, Chongqing Institute of Green and Intelligent Technology, CAS, Chongqing, China

obtaining the concept's intension and applications to image segmentation are conducted to evaluate this method. The results show the stability and performance of our method.

Keywords Cognitive transformation · Gaussian cloud model · Forward Gaussian cloud transformation · Backward Gaussian cloud transformation · Mean squared error · Image segmentation

1 Introduction

Uncertainty computing is an important feature of human cognition process. Uncertainty is a term used in subtly different ways in a number of fields, such as physics, philosophy, statistics, economics, finance, psychology, sociology, engineering, artificial intelligence, etc. [1, 16, 19, 33, 51]. In uncertainty knowledge representation field, there have been many theories and methods developed in the past decades [11, 16, 22, 48]. Probability theory studies the randomness in the way of probability and statistics and becomes an important branch of mathematics [12, 39]. Fuzzy sets proposed by Zadeh study the fuzzy membership relationship between a set and element based on fuzzy logic [46, 47]. Considering the relationship between fuzzy set and probability theory, Hirota introduced the concept of probabilistic sets [10]. Rough sets proposed by Pawlak deal with vagueness and incompleteness based on knowledge classification and uses upper and lower approximation set to define a rough concept [28, 29]. There are some uncertain theories, such as interval analysis [25], gray system [5], set pair analysis [52], extenics [3], etc. The representation and processing of uncertain knowledge are key issues, especially the randomness and the fuzziness hidden in knowledge [16, 34], and many concepts simultaneously contain randomness and fuzziness.

Human cognition process is based on language, and concept could be considered as a basic unit of natural language. The cognition of uncertain concepts is easy for human thinking, and the mutual cognitive transformation between the intension and the extension of a concept can be conducted automatically in human brain, while it is very difficult for computer since the uncertain concepts are hard to be precisely defined. For example, people do not need to know the precise extensions for many concepts, such as "young," "tall," "beautiful," etc., but it is not affected people's understanding for their intensions [18].

Gaussian cloud model (GCM) based on quadratic Gaussian distribution and Gaussian membership function provided a method to realize the bidirectional cognitive transformation between the intension and the extension of a concept through two cloud transformations, namely forward Gaussian cloud transformation (FGCT) and backward Gaussian cloud transformation (BGCT) [16, 18, 35, 36], where FGCT is used to transform the concept intention into extension, while BGCT transforms the extension into intension of a concept. Furthermore, GCM with universality can depict the transition from Gaussian distribution to heavy-tail distribution (e.g., power-law distribution), which reflects the self-similar and scale-free properties in the nature and human society [17, 44]. Therefore, GCM has been applied to many fields successfully, such as intelligent control [15], data mining [38], system evaluation [24], image segmentation [7, 30, 41], and so on [6, 42, 43, 49, 53].

In GCM, the BGCT algorithm is essentially to obtain the estimates of concept intension from random sample, so there exists the errors inevitably. At present, there are two main BGCT algorithms proposed by Liu and Wang respectively [20, 37]. However, they have some defects. In the paper, we mainly study the backward Gaussian cloud cognitive transformation algorithm based on probability statistics, analyze the defects of the existing BGCT algorithms, and propose an effective BGCT algorithm to extract concepts' intension from sample data, which is a key step for obtaining the stable concept intension in the cognitive process from extension to intension. Finally, some comparison experiments on obtaining the concept's intension and applications to image segmentation have done to evaluate this method, and the results show the stability and performance of our method.

The remainder of this paper is organized as follows. Section 2 introduces the definition and the mathematical properties of the GCM. In Section 3, the errors of the existing BGCT algorithms are analyzed in detail. In Section 4, a new BGCT algorithm is proposed and the reasonableness is also analyzed and proved in detail, while the some comparative experiments and applications to image segmentation are shown in Section 5. Final remarks and future perspectives appear in Section 6.

2 Gaussian cloud model

2.1 The definition of GCM

Gaussian distribution can be expressed by two parameters, expectation (denoted as Ex) and standard variance (σ), while Gaussian cloud model suggests using three parameters (Ex, En, He) to depict the distribution of a concept, the three parameters (Ex, En, He) are also used to represent the intension of the concept. Meanwhile, the degree of membership of an object x belonging to a concept should not be a precise value but multiple values with stable tendency within a certain range in view of the fact that a concept usually has different meanings for different people [16, 23]. For example, the concept "young" is expressed as $(Ex = 25, En = 3, He = 0.3)$, wherein $Ex = 25$ is an expected age about "young," En is the expected value of random variable σ and He is the standard variance of σ if the standard variance σ of a membership degree is not a constant, but a random variable with stable tendency. En and He are used to express the differences among people's cognition on the concept "young." Therefore, Gaussian cloud model based on Gaussian distribution and Gaussian membership degree is defined as follows [16].

Definition 1 ([16]) Let U be an universal set described by precise numbers, and C be the qualitative concept containing three numerical characters (Ex, En, He) related to U. If there is a number $x \in U$, which is a random realization of the concept C and satisfies $x = R_N(Ex, |y|)$, where $y = R_N(En, He)$, and the membership degree $\mu(x)$ with stable tendency of x on U is

$$\mu(x) = \exp\left\{-\frac{(x - Ex)^2}{2y^2}\right\}, \tag{2.1}$$

then the distribution of x on U is a *Gaussian cloud*, and each x with membership degree $\mu(x)$ is defined as a cloud drop. Where $y = R_N(En, He)$ denoted a Gaussian random number with expectation En and standard variance He.

In Definition 1, "qualitative concept" is some kind of uncertain concept in natural language, such as "young," "beauty," "maybe," and so on. "Precise number" is used to distinguish it with fuzzy number, for example, the "precise number" corresponding to the concept "young" is $\{\cdots, 17, 17.5, 18, 20, 22.5, 25, 30, \cdots\}$. While each x ($x \in U$) with membership degree μ is defined as a "cloud drop," which is different from "precise number." For further information, see the reference [16, 18]. The key point in definition 1 is the second-order relationship, i.e., within the two Gaussian random numbers $y = R_N(En, He)$ and $x = R_N(Ex, |y|)$. If $He = 0$, then the distribution of x on U will become a Gaussian distribution $N(Ex, En)$. If $He = 0$, $En = 0$, then x will be a constant Ex and $\mu(x) \equiv 1$. When He turns larger, the distribution of random variable X will show a heavier tail, which can be used in economic and social researches [8].

2.2 The mathematical properties of GCM

Let U be an universal set, and define random variable X and Y on U, then the probability density function of random variable Y from definition 1 is

$$f_Y(y) = \frac{1}{\sqrt{2\pi}He} e^{-\frac{(y-En)^2}{2He^2}}. \tag{2.2}$$

Considering $Y = y$, the conditional probability density function of Gaussian cloud random variable X is

$$f_{X|Y}(x|Y = y) = \frac{1}{\sqrt{2\pi}|y|} e^{-\frac{(x-Ex)^2}{2y^2}}. \tag{2.3}$$

Based on the conditional probability density: $f_{X,Y}(x, y) = f_{X|Y}(x|Y = y) f_Y(y)$, the probability density function of Gaussian cloud random variable X is

$$f_X(x) = \int_{-\infty}^{+\infty} f_{X,Y}(x, y)dy = \frac{1}{2\pi He} \int_{-\infty}^{+\infty} \frac{1}{|y|} e^{-\frac{(x-Ex)^2}{2y^2} - \frac{(y-En)^2}{2He^2}} dy. \tag{2.4}$$

The expected value, variance (second-order central moment), third-order central moment, and fourth-order central moment of Gaussian cloud random variable X can be obtained as follows [21, 37].

(1) $\mathrm{E}X = Ex$;
(2) $\mathrm{D}X = En^2 + He^2$;
(3) $\mathrm{E}(X - Ex)^3 = 0$;
(4) $\mathrm{E}(X - Ex)^4 = 3(3He^4 + 6He^2En^2 + En^4)$.

3 Gaussian cloud transformation algorithm and analysis

A concept is composed of its intension and extension, where the intension refers to the sum of the essential attributes of a concept reflecting the nature of things, that is, the content of the concept, while the extension refers to the set of all instances of the concept. In Gaussian cloud model, the intension of a concept is depicted by the numerical characteristics (Ex, En, He), and its extension is the set of all the cloud drops with different membership degrees. Furthermore, the mutual cognitive transformation between intension and extension of a concept is implemented by Gaussian cloud transformation, including forward Gaussian cloud transformation (FGCT) and backward Gaussian cloud transformation (BGCT), where FGCT is used to realize the cognitive transformation from intension to extension of a concept, and BGCT implements the cognitive transformation from extension to intension. The two Gaussian cloud transformations also provide a way to simulate the human cognition process for concepts by computer. Therefore, we can use the numerical characteristics of a concept to generate cloud drop with different membership degrees by devising FGCT algorithm. Similarly, BGCT algorithm can be also devised to obtain the intension of a concept from cloud drops or sample data.

3.1 FGCT algorithm

Based on the Definition 1, the FGCT algorithm, which provides a method to transform a qualitative concept with Ex, En, and He into a number of cloud drops (i.e., the extension of concept), can be obtained as follows [16].

Algorithm 1 [16] FGCT

Input: (Ex, En, He) and the number of cloud drops n.
Output: n cloud drops x_i and their membership degrees $\mu(x_i)$, $i = 1, 2, \cdots, n$.
Step1: Generate a Gaussian random number y_i with expectation En and standard variance He, i.e., $y_i = R_N(En, He)$.
Step2: Generate a Gaussian random number x_i with expectation Ex and standard variance $|y_i|$, i.e., $x_i = R_N(Ex, |y_i|)$.
Step3: Calculate membership degree $\mu(x_i) = \exp\left\{-\frac{(x_i - Ex)^2}{2y_i^2}\right\}$.
Step4: x_i with membership degree $\mu(x_i)$ is a cloud drop in the domain.
Step5: Repeat step1 to step4 until n cloud drops are generated.

For example, different people have different understanding about the uncertain concept "young," so it is very difficult to give a crisp membership degree. If the concept “young” is expressed as ($Ex = 25$, $En = 3$, $He = 0.3$), then the “young” is converted into some cloud drops representing ages about “young” with different membership degrees by FGCT algorithm. The cloud map is shown in Fig. 1, which show that each age(cloud drop) x has more than one membership degree.

Cloud drops can be used to describe a commonsense concept extension, while the numerical characteristics Ex, En, He obtained by BGCT can be used to describe the commonsense concept intension. Gaussian cloud model just uses FGCT and BGCT to realize the bidirectional cognitive transformation between the intension and extension of a qualitative concept.

3.2 BGCT algorithm

Corresponding to the FGCT, BGCT is to get the estimates of (Ex, En, He). So some methods of statistic inference is often used in BGCT, where the point estimate is a method to obtain the estimates of unknown parameters using a specific value. The point estimate method mainly has moment estimation and maximum likelihood estimation. As the probability density function $f_X(x)$ (see (2.4)) of Gaussian cloud random variable X does not have analytical form, it is difficult to estimate Ex, En, and He if we use maximum likelihood estimation. Therefore, the moment estimation is often used in BGCT. There are two main BGCT methods which are used to estimate Ex, En, and He based on the method of moments. One is proposed by Li and Liu based on the sample variance and the sample first-order absolute central moment [16, 20]. Another is proposed by Wang according to the sample variance and the sample fourth-order central moment [37].

3.2.1 The BGCT algorithm based on the sample 1st-order absolute central moment

As this method obtains the estimators $(\hat{E}x, \hat{E}n, \hat{H}e)$ of (Ex, En, He) from random sample through the single-step directly, the BGCT algorithm based on the sample

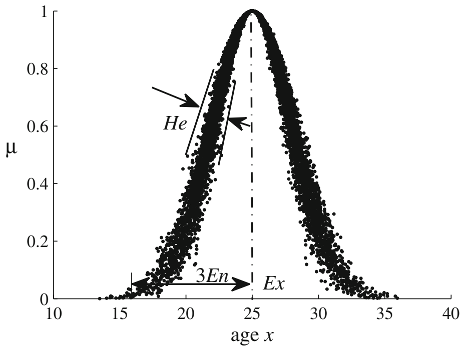

Fig. 1 Describe “young” by GCM

1st-order absolute central moment is denoted as SBGCT-1stM. The specific steps are displayed in Algorithm 2.

Algorithm 2 [20] SBGCT-1stM

Input: The random sample $X_1, X_2, \cdots, X_n$ with sample size n from a population.
Output: The estimators $(\hat{E}x, \hat{E}n, \hat{H}e)$ representing a qualitative concept.

Step1: Calculate the sample mean, the sample variance, and the sample first-order absolute central moment from the random sample $X_1, X_2, \cdots, X_n$. Namely,

$$\bar{X} = \frac{1}{n}\sum_{i=1}^{n} X_i, \quad S^2 = \frac{1}{n-1}\sum_{i=1}^{n}(X_i - \bar{X})^2, \quad M|X - \bar{X}| = \frac{1}{n}\sum_{i=1}^{n}\left|X_i - \bar{X}\right|.$$

Step2: According to the statistical properties of Gaussian cloud distribution, i.e.,

$$\begin{cases} \mathrm{E}X = Ex, \\ \mathrm{E}|X - \mathrm{E}X| = \sqrt{\frac{2}{\pi}}En, \\ \mathrm{D}X = He^2 + En^2. \end{cases} \tag{3.1}$$

Equate the sample moments to the corresponding population moments, i.e.,

$$\begin{cases} \mathrm{E}X = Ex = \bar{X}, \\ \mathrm{E}|X - \mathrm{E}X| = \sqrt{\frac{2}{\pi}}En = M|X - \bar{X}|, \\ \mathrm{D}X = He^2 + En^2 = S^2. \end{cases} \tag{3.2}$$

Calculate the estimators $\hat{E}x$, $\hat{E}n$ and $\hat{H}e$ from (3.2), i.e.,

$$\hat{E}x = \bar{X}, \quad \hat{E}n = \sqrt{\frac{\pi}{2}} \times \frac{1}{n}\sum_{i=1}^{n}|X_i - \bar{X}|, \quad \hat{H}e = \sqrt{S^2 - \hat{E}n^2}.$$

Calculate the estimates $\hat{E}x$, $\hat{E}n$, and $\hat{H}e$ based on SBGCT-1stM algorithm for the specific sample values $x_1, x_2, \cdots, x_n$. However, in (3.1), the first absolute central moment $\mathrm{E}|X - \mathrm{E}X| = \sqrt{\frac{2}{\pi}}En$ presented by Liu is not completely correct. In fact, by probability density function of Gaussian cloud X (see (2.4)), we have

$$\begin{aligned} \mathrm{E}|X - \mathrm{E}X| &= \int_{-\infty}^{+\infty} |x - Ex| f_X(x)dx \\ &= \frac{1}{2\pi He}\int_{-\infty}^{+\infty}\int_{-\infty}^{+\infty} |x - Ex| \frac{1}{|y|} e^{-\frac{(x-Ex)^2}{2y^2} - \frac{(y-En)^2}{2He^2}} dxdy, \end{aligned} \tag{3.3}$$

where, we get

$$\int_{-\infty}^{+\infty} |x - Ex| \frac{1}{|y|} e^{-\frac{(x-Ex)^2}{2y^2}} dx = 2|y|. \tag{3.4}$$

Thus, from (3.3), $\mathrm{E}|X - \mathrm{E}X|$ is related with $|y|$.

If $y > 0$, then $\mathrm{E}|X - \mathrm{E}X| = \sqrt{\frac{2}{\pi}} En$. This is the result of SBGCT-1stM [20].

However, following the Definition 1, $y = R_N(En, He)$ is a non-zero real number. Namely, y may be a negative value. So if y is a non-zero real number, it means that the symbol of absolute value of variable y in expression (3.3) can not be removed, then we can get

$$\mathrm{E}|X - \mathrm{E}X| = \sqrt{\frac{2}{\pi}} En + 2\sqrt{\frac{2}{\pi}} \cdot \frac{1}{\sqrt{2\pi} He} \int_0^{+\infty} y e^{-\frac{(y+En)^2}{2He^2}} dy, \tag{3.5}$$

where, the expression $\frac{1}{\sqrt{2\pi} He} \int_0^{+\infty} y e^{-\frac{(y+En)^2}{2He^2}} dy > 0$.

Therefore, the (3.5) shows that the SBGCT-1stM algorithm will have a large deviation if using $\hat{E}n = \sqrt{\frac{\pi}{2}} \times \frac{1}{n} \sum_{i=1}^{n} |X_i - \bar{X}|$ to estimate En. We make a further analysis of the SBGCT-1stM algorithm. y is actually a Gaussian random number with expectation En and standard variance He since $y = R_N(En, He)$. If $3He \leq En$, then the random number y is a non-negative value with the probability 99.7% in terms of the "$3He$" principle of Gaussian distribution $N(En, He^2)$. In other words, the SBGCT-1stM algorithm will have relatively accurate estimates for En and He under the condition of $3He \leq En$. However, if $3He > En$, then the probability which the random number y is a negative will gradually increase with the increasing of the ratio He/En, which will cause that the estimate $\hat{E}n$ is greater than the true value En (see (3.5)); meanwhile, the estimate $\hat{H}e$ is less than the true value He . In addition, through experiment, we also find if the true value $He \to 0$, the estimate $\hat{H}e = \sqrt{S^2 - \hat{E}n^2}$ may be an imaginary number (see Example 1).

3.2.2 *The BGCT based on the sample 4th-order central moment*

In 2011, Wang proposed another BGCT algorithm based on the sample variance and the sample 4th-order central moment [37]. This method is also the single-step to get the estimators $(\hat{E}x, \hat{E}n, \hat{H}e)$ from sample directly, so we denote it as SBGCT-4thM. The specific steps of SBCGT-4thM are displayed in Algorithm 3.

Algorithm 3 [37] SBGCT-4thM

Input: The random sample $X_1, X_2, \cdots, X_n$ with sample size n from a population.
Output: The estimators $(\hat{E}x, \hat{E}n, \hat{H}e)$ representing a qualitative concept.

Step1: Calculate the sample mean, the sample variance, and the sample fourth-order central moment from the random sample $X_1, X_2, \cdots, X_n$, namely,

$$\bar{X} = \frac{1}{n}\sum_{i=1}^{n} X_i, \quad S^2 = \frac{1}{n-1}\sum_{i=1}^{n}(X_i - \bar{X})^2, \quad M_4 = \frac{1}{n}\sum_{i=1}^{n}(X_i - \bar{X})^4.$$

Step2: According to the statistical properties of Gaussian cloud distribution, i.e.,

$$\begin{cases} \mathrm{E}X = Ex, \\ \mathrm{D}X = He^2 + En^2, \\ \mathrm{E}(X - \mathrm{E}X)^4 = 9He^4 + 3En^4 + 18En^4He^4. \end{cases} \tag{3.6}$$

Equate the sample moments to the corresponding population moments, i.e.,

$$\begin{cases} \mathrm{E}X = Ex = \bar{X}, \\ \mathrm{D}X = He^2 + En^2 = S^2, \\ \mathrm{E}(X - \mathrm{E}X)^4 = 9He^4 + 3En^4 + 18En^2He^2 = M_4. \end{cases} \tag{3.7}$$

Calculate the estimators $\hat{E}x$, $\hat{E}n$ and $\hat{H}e$ from (3.7), i.e.,

$$\hat{E}x = \bar{X}, \ \hat{E}n = \sqrt[4]{\frac{9\left(S^2\right)^2 - M_4}{6}}, \ \hat{H}e = \sqrt{S^2 - \hat{E}n^2}. \tag{3.8}$$

In SBGCT-4thM, the key issue is to ensure the estimators $\hat{E}n^2 = \sqrt{\frac{9(S^2)^2 - M_4}{6}} \geq 0$ and $\hat{H}e^2 = S^2 - \hat{E}n^2 \geq 0$, which is equivalent to the following inequality, i.e.,

$$3\left(\frac{1}{n-1}\sum_{i=1}^{n}(X_i - \bar{X})^2\right)^2 \leq \frac{1}{n}\sum_{i=1}^{n}(X_i - \bar{X})^4 \leq 9\left(\frac{1}{n-1}\sum_{i=1}^{n}(X_i - \bar{X})^2\right)^2 \tag{3.9}$$

The inequality (3.9) is related with the sample $X_1, X_2, \cdots, X_n$ and the sample size n. Therefore, $9(S^2)^2 - M_4 < 0$ or $S^2 - \sqrt{(9\left(S^2\right)^2 - M_4)/6} < 0$ may occur in some cases, which make the estimates $\hat{E}n$ and $\hat{H}e$ not be obtained (see Example 1).

Example 1 Let $(Ex = 0, En = 1, He)$ express a concept "near zero," where He is changing from 0 to 0.5 with step by 0.01 first, and then from 0.5 to 3 with step by 0.05. The test sample is generated by FGCT ($n = 5000$). The estimates $\hat{E}n$ and $\hat{H}e$, which are calculated by SBGCT-1stM and SBGCT-4thM, are shown in Figs. 2 and 3,[1] respectively.

[1]Note: If the estimates $\hat{E}n$ and $\hat{H}e$ are imaginary numbers, we then denote $\hat{E}n = -0.5$ and $\hat{H}e = -0.5$.

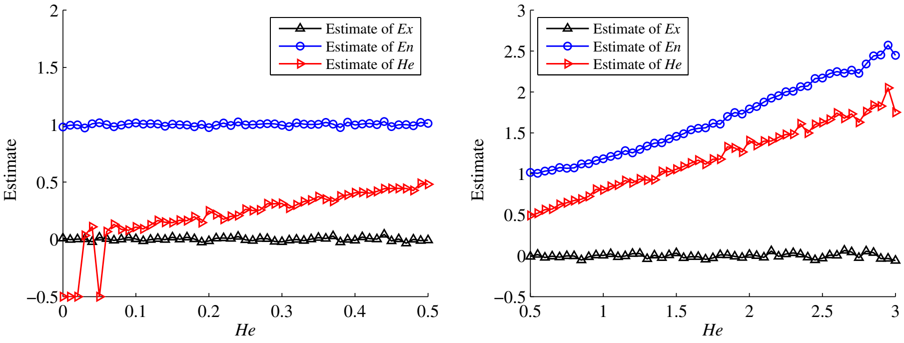

(a) He is changing with setp by 0.01 (b) He is changing with setp by 0.05

Fig. 2 The estimates of Ex, En, He with the changing of He in SBGCT-1stM

Figures 2 and 3 show that the estimate $\hat{H}e$ may be an imaginary number in SBGCT-1stM and SBGCT-4thM if $He \to 0$, see Figs. 2a and 3a; the estimate $\hat{E}n$ is larger than the true value En and the estimate $\hat{H}e$ is less than the true value He if $En < 3He$ in SBGCT-1stM, see Fig. 2b; the inequality (3.9) may not hold for some sample values, see Fig. 3b.

Therefore, the results of Example 1 show that SBGCT-1stM and SBCGT-4thM exist some drawbacks. In this work, we propose a new method which can overcome above drawbacks. The specific contents will be illustrated in Section 4.

4 Multi-step backward gaussian cloud transformation algorithm and its error analysis

According to FGCT, each cloud drop x_i is generated by two times Gaussian random, that is, $y_i = R_N(En, He)$, $x_i = R_N(Ex, |y_i|)$, and y_i is the input to generate x_i.

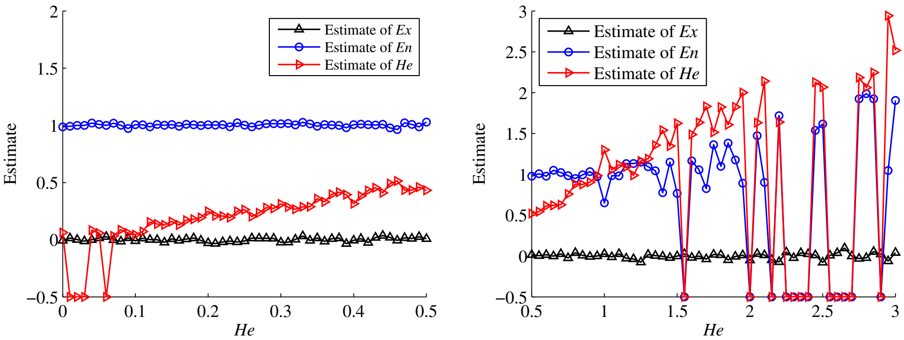

(a) He is changing with setp by 0.01 (b) He is changing with setp by 0.05

Fig. 3 The estimates of Ex, En, He with the changing of He in SBGCT-4thM

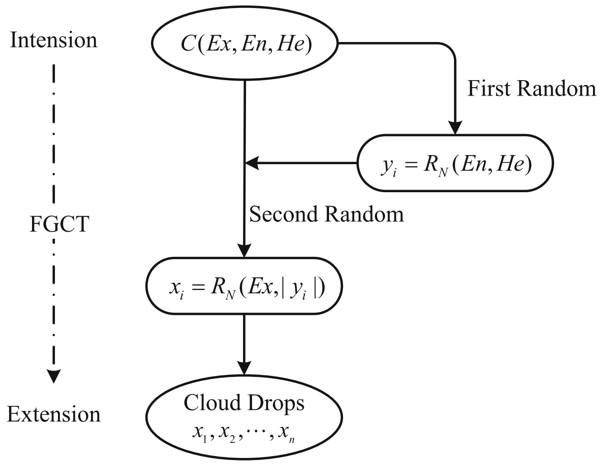

Fig. 4 The process of cloud drops generated by FGCT

Thus, n cloud drops $x_1, x_2, \cdots, x_n$ are obtained by multiple cycles. The detailed process of FGCT is shown in Fig. 4. In addition, the FGCT is a cognitive transformation process from concept's intension with (Ex, En, He) to a lot of quantitative numbers, while the BGCT is a cognitive transformation from some sample data into a concept's intention with (Ex, En, He), which means that the FGCT and the BGCT are the two mutually inverse processes. So, based on the features of cloud drops obtained by two steps, (Ex, En, He) should be estimated from sample data through the multi-step rather than the single-step. Whereby, we propose a multi-step BGCT algorithm.

4.1 MBGCT-SD algorithm

From Fig. 4, n cloud drops $x_i = R_N(Ex, |y_i|)$ are related with Ex and y_i directly, while $y_i = R_N(En, He)$ is related with En and He directly, or, to say that n cloud drops x_i are related with En and He indirectly, $i = 1, 2, \cdots, n$. So, the estimate $\hat{E}x$ can be obtained by $x_1, x_2, \cdots, x_n$ directly, but the estimates $\hat{E}n$ and $\hat{H}e$ are not. However, the estimates $\hat{E}n$ and $\hat{H}e$ can be obtained by a group of values $y_1, y_2, \cdots, y_m$, where, $y_1, y_2, \cdots, y_m$ can be calculated separately by m groups of sample which are obtained by sample division from $x_1, x_2, \cdots, x_n$. So we call it multi-step BGCT algorithm based on sample division, denoted as MBGCT-SD. The specific process of MBGCT-SD is shown in Fig. 5 and the detailed steps are displayed in Algorithm 4.

In MBGCT-SD,[2] expression (4.2) can be described by Theorem 1.

[2]Note: If $r = 1$, there is only one sample X_{k1} in each group sample, so, $Y_k^2 = 0$ $(k = 1, 2, \cdots, m)$, then $\hat{E}n = \hat{H}e = 0$; If $m = 1$, there is only one group sample, then $\hat{E}n^2 = \hat{E}Y^2 = Y_1^2$, $\hat{H}e^2 = 0(\hat{D}Y^2 = 0)$.

Algorithm 4 MBGCT-SD

Input: The random sample $X_1, X_2, \cdots, X_n$ with sample size n from a population.
Output: The estimators $(\hat{E}x, \hat{E}n, \hat{H}e)$ representing a qualitative concept.

Step1: Make the sample mean from the random sample $X_1, X_2, \cdots, X_n$ as the estimator of Ex, i.e.,

$$\hat{E}x = \bar{X} = \frac{1}{n}\sum_{i=1}^{n} X_i.$$

Step2: Draw m groups of samples without replacement from $X_1, X_2, \cdots, X_n$ randomly, denoted as $X_{11}, X_{12}, \cdots, X_{1r}; X_{21}, X_{22}, \cdots, X_{2r}; \cdots; X_{m1}, X_{m2}, \cdots, X_{mr}$, where, r represents the requited sample size per group. Whereafter, calculate the sample variance of each group of sample, namely,

$$Y_k^2 = \frac{1}{r-1}\sum_{j=1}^{r}\left(X_{kj} - \bar{X}_k\right)^2, k = 1, 2, \cdots, m. \tag{4.1}$$

where, $\bar{X}_k = \frac{1}{r}\sum\limits_{j=1}^{r} X_{kj}$ is sample mean of the kth group sample.

Let data set $Y^2 = \left\{Y_1^2, Y_2^2, \cdots, Y_m^2\right\}$.

Step3: Calculate the estimators $\hat{E}n^2$ and $\hat{H}e^2$ from data set Y^2, i.e.,

$$\hat{E}n^2 = \frac{1}{2}\sqrt{4[\hat{\mathrm{E}}Y^2]^2 - 2\hat{\mathrm{D}}Y^2},\ \hat{H}e^2 = \hat{\mathrm{E}}Y^2 - \hat{E}n^2. \tag{4.2}$$

Where, $\hat{\mathrm{E}}Y^2 = \frac{1}{m}\sum\limits_{k=1}^{m} Y_k^2$ and $\hat{\mathrm{D}}Y^2 = \frac{1}{m-1}\sum\limits_{k=1}^{m}\left(Y_k^2 - \hat{\mathrm{E}}Y^2\right)^2$ represent the sample mean and the sample variance of Y^2, respectively.

Theorem 1 *Let $Y_1, Y_2, \cdots Y_m$ be independent and identically distributed random sample from the Gaussian population $Y \sim N(En, He^2)$, then the expression (4.2) can be obtained.*

Proof Following the formula (2.2), if $Y \sim N(En, He^2)$, then we have

$$\mathrm{E}Y^2 = \int_{-\infty}^{+\infty} y^2 f_Y(y)dy = He^2 + En^2. \tag{4.3}$$

$$\mathrm{E}Y^4 = \int_{-\infty}^{+\infty} y^4 f_Y(y)dy = 3He^4 + 6En^2He^2 + En^4.$$

Thus,

$$\mathrm{D}Y^2 = \mathrm{E}Y^4 - (\mathrm{E}Y^2)^2 = 2He^4 + 4En^2He^2. \tag{4.4}$$

Equate the sample moments to the corresponding population moments, we then have

$$\begin{cases} \mathrm{E}Y^2 = He^2 + En^2 = \hat{\mathrm{E}}Y^2, \\ \mathrm{D}Y^2 = 2He^4 + 4En^2He^2 = \hat{\mathrm{D}}Y^2. \end{cases} \tag{4.5}$$

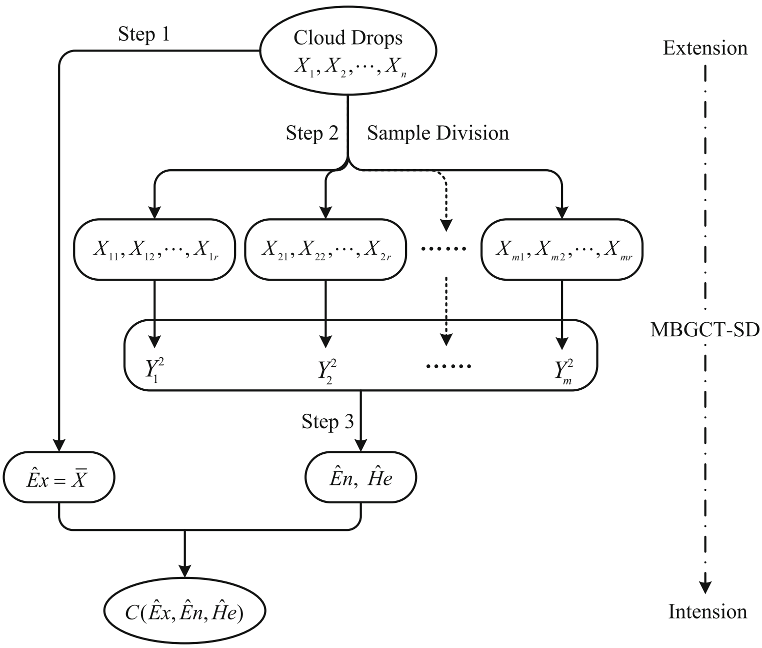

Fig. 5 The process of MBGCT-SD

where, $\hat{\mathrm{E}}Y^2 = \frac{1}{m}\sum_{k=1}^{m} Y_k^2$ and $\hat{\mathrm{D}}Y^2 = \frac{1}{m-1}\sum_{k=1}^{m}\left(Y_k^2 - \hat{\mathrm{E}}Y^2\right)^2$ represent the sample mean and the sample variance of Y^2, respectively.

From the (4.5), we obtain

$$2He^4 - 4\hat{\mathrm{E}}Y^2He^2 + \hat{\mathrm{D}}Y^2 = 0. \tag{4.6}$$

This is a quadratic equation about He^2. We can get the discriminant of root from (4.6), i.e.,

$$\Delta = 16(\hat{\mathrm{E}}Y^2)^2 - 8\hat{\mathrm{D}}Y^2, \tag{4.7}$$

where,

$$16(\hat{\mathrm{E}}Y^2)^2 - 8\hat{\mathrm{D}}Y^2 = 16(\hat{\mathrm{E}}Y^2)^2 - \frac{8}{m-1}\sum_{k=1}^{m}\left(\hat{\mathrm{E}}Y^2 - Y_k^2\right)^2 \geq 16(\hat{\mathrm{E}}Y^2)^2$$
$$-\frac{8}{m-1}\sum_{k=1}^{m}(\hat{\mathrm{E}}Y^2)^2 = \frac{8(m-2)}{m-1}(\hat{\mathrm{E}}Y^2)^2.$$

Thus, $\Delta = 16(\hat{\mathrm{E}}Y^2)^2 - 8\hat{\mathrm{D}}Y^2 \geq 0$ if $m \geq 2$.

Hence, from the (4.5), we get two groups of solutions, i.e.,

$$En_1^2 = \frac{\sqrt{\Delta}}{4}, \quad He_1^2 = \frac{4\hat{\mathrm{E}}Y^2 - \sqrt{\Delta}}{4};$$
$$En_2^2 = -\frac{\sqrt{\Delta}}{4}, \quad He_2^2 = \frac{4\hat{\mathrm{E}}Y^2 + \sqrt{\Delta}}{4} \text{ (Discarded)}.$$

En_2^2 and He_2^2 are discarded since $En_2^2 < 0$. Thus, En_1^2 and He_1^2 are the estimators $\hat{E}n^2$ and $\hat{H}e^2$ in expression (4.2). □

From the expression (4.2), $\hat{E}n$ and $\hat{H}e$ can be obtained, and $\hat{E}n > 0$, $\hat{H}e > 0$. So, the MBGCT-SD algorithm can ensure that $\hat{E}n$ and $\hat{H}e$ will not be imaginary numbers. We next analyze the mean and mean squared error (MSE) of estimators $\hat{E}x$, $\hat{E}n$ and $\hat{H}e$ in detail.

4.2 Evaluation of estimators $\hat{E}x$, $\hat{E}n$, and $\hat{H}e$

According to statistical principles [4], the more samples there are, the less the error in the BGCT algorithm will be. Due to the constraint of sample size, the error exists no matter what algorithm is used. As the BGCT algorithms are based on the statistical result of a large number of cloud drops, the performance is determined by the number of drops. In general, the errors of three parameters will decrease as the number of cloud drops increasing.

An estimator is a function of the sample, while an estimate is the realized value of an estimator (that is, a number) that is obtained when a sample is actually taken. Notationally, when a sample is taken, an estimator is a function of the random variables $X_1, X_2, \cdots, X_n$, while an estimate is function of the realized values $x_1, x_2, \cdots, x_n$. So the estimators $\hat{E}x$, $\hat{E}n$, and $\hat{H}e$ are three functions about random variables and they will have different estimates for different sample values. These estimates will be biased for the true value. But when these estimators are reused many times, we expect that the mean of these estimates will equal to the true value of unknown parameters. In addition, we need to calculate the mean squared error (MSE) of estimator in order to reflect the differences between the estimator and the true value. Thus, we next analyze the mean and MSE of estimators $\hat{E}x$, $\hat{E}n$, and $\hat{H}e$. Firstly, we present the following definition and inequalities.

Definition 2 ([4]) The mean squared error (MSE) of an estimator $\hat{\theta}$ of a parameter θ is the function of θ defined by $\mathrm{MSE}(\hat{\theta}) = \mathrm{E}(\hat{\theta} - \theta)^2$.

MSE has at least two advantages over other distance measures [4]: First, it is quiet tractable analytically and, second, it has the interpretation

$$\mathrm{MSE}(\hat{\theta}) = \mathrm{E}(\hat{\theta} - \theta)^2 = \mathrm{D}\hat{\theta} + (\mathrm{E}\hat{\theta} - \theta)^2,$$

where, $\mathrm{D}\hat{\theta}$ is the variance of estimator $\hat{\theta}$, and $\mathrm{E}\hat{\theta} - \theta$ is the bias of estimator $\hat{\theta}$. If $\mathrm{E}\hat{\theta} - \theta = 0$, then $\hat{\theta}$ is unbiased estimator of θ. The unbiasedness [4] is an important requirement for an estimator.

Theorem 2 ([4] (Hölder's Inequality)) *Let X be an any random variable, then*

$$\mathrm{E}\,|X| \le \{\mathrm{E}|X|^p\}^{1/p}, \quad 1 < p < \infty.$$

Theorem 3 ([4] (Liapounov's Inequality)) *Let X be an any random variable, then*

$$\{\mathrm{E}|X|^r\}^{1/r} \le \{\mathrm{E}|X|^s\}^{1/s}, \quad 1 < r < s < \infty.$$

Theorem 4 ([4] (Jensen's Inequality)) *For any random variable X, if $g(x)$ is a convex function, then*

$$\mathrm{E}g(X) \ge g(\mathrm{E}X),$$

and if $g(x)$ is a concave function, then

$$\mathrm{E}g(X) \le g(\mathrm{E}X).$$

Equality holds if and only if, for every line $a + bx$ that is tangent to $g(x)$ at $x = \mathrm{E}X$, $P(g(x) = a + bX) = 1$.

The mean and the MSE of estimators $\hat{E}x, \hat{E}n$ and $\hat{H}e$ will have the next conclusions.

Theorem 5 *Let $X_1, X_2, \cdots, X_n$ be a random sample from a population. Then the mean of estimator $\hat{E}x$ is*

$$\mathrm{E}(\hat{E}x) = Ex,$$

and its MSE *satisfies*

$$\mathrm{MSE}(\hat{E}x) = \mathrm{E}(\hat{E}x - Ex)^2 = \frac{1}{n}(He^2 + En^2). \tag{4.8}$$

Proof From the step 1 of MBGCT-SD, we have

$$\mathrm{E}(\hat{E}x) = \frac{1}{n}\mathrm{E}\sum_{i=1}^{n} X_i = \frac{1}{n}\sum_{i=1}^{n} \mathrm{E}X_i,$$

$$\mathrm{MSE}(\hat{E}x) = \mathrm{D}(\hat{E}x) + (\mathrm{E}(\hat{E}x) - Ex)^2 = \frac{1}{n^2}\sum_{i=1}^{n} \mathrm{D}X_i + (\mathrm{E}(\hat{E}x) - Ex)^2.$$

Considering the statistical properties of Gaussian cloud model, we get

$$\mathrm{E}X = Ex, \quad \mathrm{D}X = He^2 + En^2.$$

Thus, $\mathrm{E}(\hat{E}x) = Ex$, $\mathrm{MSE}(\hat{E}x) = \frac{1}{n}(He^2 + En^2)$. □

Theorem 6 *The mean of estimator $\hat{E}n^2$ is*

$$\mathrm{E}(\hat{E}n^2) = \sqrt{\frac{r}{n}\mathrm{D}Y^2 + En^4}, \tag{4.9}$$

and its MSE *is*

$$\mathrm{MSE}(\hat{E}n^2) = \mathrm{E}(\hat{E}n^2 - En^2)^2 = \frac{r}{n}\mathrm{D}Y^2 + 2En^4 - 2En^2\sqrt{\frac{r}{n}\mathrm{D}Y^2 + En^4}. \quad (4.10)$$

where, $\mathrm{D}Y^2 = 2He^2(He^2 + 2En^2)$.

Proof From Definition 2, we have

$$\mathrm{MSE}(\hat{E}n^2) = \mathrm{E}(\hat{E}n^2 - En^2)^2 = \mathrm{E}(\hat{E}n^4) - 2En^2 \cdot \mathrm{E}(\hat{E}n^2) + En^4. \quad (4.11)$$

So, we need compute $\mathrm{E}(\hat{E}n^4)$ and $\mathrm{E}(\hat{E}n^2)$. Following the expression (4.2), $\hat{E}n^4 = (\hat{\mathrm{E}}Y^2)^2 - \frac{1}{2}\hat{\mathrm{D}}Y^2$. Thus,

$$\mathrm{E}(\hat{E}n^4) = \mathrm{E}(\hat{\mathrm{E}}Y^2)^2 - \frac{1}{2}\mathrm{E}(\hat{\mathrm{D}}Y^2).$$

Since, $\hat{\mathrm{E}}Y^2 = \frac{1}{m}\sum_{k=1}^{m} Y_k^2$, $\hat{\mathrm{D}}Y^2 = \frac{1}{m-1}\sum_{k=1}^{m}\left(Y_k^2 - \hat{\mathrm{E}}Y^2\right)^2$. Then

$$\begin{aligned}\mathrm{E}(\hat{\mathrm{E}}Y^2)^2 &= \mathrm{D}(\hat{\mathrm{E}}Y^2) + \mathrm{E}(\hat{\mathrm{E}}Y^2))^2 = \mathrm{D}\left(\frac{1}{m}\sum_{k=1}^{m} Y_k^2\right) + \left(\mathrm{E}(\frac{1}{m}\sum_{k=1}^{m} Y_k^2)\right)^2\\ &= \frac{1}{m}\mathrm{D}Y^2 + (\mathrm{E}Y^2)^2,\\ {}^{3}\mathrm{E}(\hat{\mathrm{D}}Y^2) &= \mathrm{E}\left(\frac{1}{m-1}\sum_{k=1}^{m}\left(Y_k^2 - \hat{\mathrm{E}}Y^2\right)^2\right) = \mathrm{D}Y^2.\end{aligned}$$

Therefore, from the (4.5) and $n = m \cdot r$, we get

$$\mathrm{E}(\hat{E}n^4) = \frac{1}{m}\mathrm{D}Y^2 + \left(\mathrm{E}Y^2\right)^2 - \frac{1}{2}\mathrm{D}Y^2 = \frac{r}{n}\mathrm{D}Y^2 + En^4. \quad (4.12)$$

In addition, by Theorem 3, we have $\{\mathrm{E}(\hat{E}n^2)\}^{1/2} \leq \{\mathrm{E}(\hat{E}n^4)\}^{1/4} = \left(\frac{r}{n}\mathrm{D}Y^2 + En^4\right)^{1/4}$, i.e.,

$$\mathrm{E}(\hat{E}n^2) \leq \sqrt{\frac{r}{n}\mathrm{D}Y^2 + En^4}. \quad (4.13)$$

On the other hand, as $g(x) = \sqrt{x}$ is a convex function, from Theorem 4 and the expression (4.12), we have

$$\mathrm{E}(\hat{E}n^2) = \frac{1}{2}\mathrm{E}\sqrt{4\left(\hat{\mathrm{E}}Y^2\right)^2 - 2\hat{\mathrm{D}}Y^2} \geq \frac{1}{2}\sqrt{\mathrm{E}(4\left(\hat{\mathrm{E}}Y^2\right)^2 - 2\hat{\mathrm{D}}Y^2)} = \frac{1}{2}\sqrt{\mathrm{E}(4\hat{E}n^4)}.$$

So,

$$\mathrm{E}(\hat{E}n^2) \geq \sqrt{\frac{r}{n}\mathrm{D}Y^2 + En^4}. \quad (4.14)$$

[3] The sample variance is unbiased estimate of variance.

Thus, following the expressions (4.13) and (4.14), we have $\mathrm{E}(\hat{E}n^2) = \sqrt{\frac{r}{n}\mathrm{D}Y^2 + En^4}$.

Finally, applying $\mathrm{E}(\hat{E}n^2)$ and $\mathrm{E}(\hat{E}n^4)$ into the expression (4.11), we obtain $\mathrm{MSE}(\hat{E}n^2)$. □

Theorem 7 *If the estimator $\hat{E}n$ is non-negative, then the mean of estimator $\hat{E}n$ is*

$$\mathrm{E}(\hat{E}n) = [\mathrm{E}(\hat{E}n^2)]^{1/2} = \left(\frac{r}{n}\mathrm{D}Y^2 + En^4\right)^{1/4}, \tag{4.15}$$

and its MSE *is*

$$\mathrm{MSE}(\hat{E}n) = \sqrt{\frac{r}{n}\mathrm{D}Y^2 + En^4} - 2En \cdot \left(\frac{r}{n}\mathrm{D}Y^2 + En^4\right)^{1/4} + En^2. \tag{4.16}$$

Proof If the estimator $\hat{E}n$ is non-negative, then from Theorem 2, we have $\mathrm{E}(\hat{E}n) \leq [\mathrm{E}(\hat{E}n^2)]^{1/2}$. As $g(x) = x^2$ is a concave function, from Theorem 4, we get $\mathrm{E}(\hat{E}n^2) \leq [\mathrm{E}(\hat{E}n)]^2$, that is, $\mathrm{E}(\hat{E}n) \geq [\mathrm{E}(\hat{E}n^2)]^{1/2}$. Thus, from Theorem 6, we obtain the expression (4.15).

In addition, the MSE of estimator $\hat{E}n$ is

$$\mathrm{MSE}(\hat{E}n) = \mathrm{E}(\hat{E}n - En)^2 = \mathrm{E}(\hat{E}n^2) - 2En \cdot \mathrm{E}(\hat{E}n) + En^2. \tag{4.17}$$

Applying $\mathrm{E}(\hat{E}n)$ and $\mathrm{E}(\hat{E}n^2)$ into the expression (4.17), we obtain $\mathrm{MSE}(\hat{E}n)$. □

Theorem 8 *The mean of estimator $\hat{H}e$ is*

$$\mathrm{E}(\hat{H}e) = \left(He^2 + En^2 - \sqrt{\frac{r}{n}\mathrm{D}Y^2 + En^4}\right)^{1/2}, \tag{4.18}$$

and its MSE *is*

$$\begin{aligned}\mathrm{MSE}(\hat{H}e) &= 2He^2 + En^2 - \sqrt{\frac{r}{n}\mathrm{D}Y^2 + En^4} \\ &\quad -2He\left(He^2 + En^2 - \sqrt{\frac{r}{n}\mathrm{D}Y^2 + En^4}\right)^{1/2}.\end{aligned} \tag{4.19}$$

Proof From the expression (4.2), we have $\mathrm{E}(\hat{H}e) = \mathrm{E}\sqrt{\hat{\mathrm{E}}Y^2 - \hat{E}n^2}$. Since $g(x) = \sqrt{x}$ is a convex function, from Theorem 4, we get

$$\mathrm{E}(\hat{H}e) = \mathrm{E}\sqrt{\hat{\mathrm{E}}Y^2 - \hat{E}n^2} \geq \sqrt{\mathrm{E}(\hat{\mathrm{E}}Y^2 - \hat{E}n^2)} = \sqrt{\mathrm{E}Y^2 - \mathrm{E}(\hat{E}n^2)}.$$

Furthermore, according to the Theorem 2, we have

$$\mathrm{E}(\hat{H}e) = \mathrm{E}\sqrt{\hat{\mathrm{E}}Y^2 - \hat{E}n^2} \leq \left[\mathrm{E}\left(\sqrt{\hat{\mathrm{E}}Y^2 - \hat{E}n^2}\right)^2\right]^{1/2} = \sqrt{\mathrm{E}Y^2 - \mathrm{E}(\hat{E}n^2)}.$$

So, we obtain

$$\mathrm{E}(\hat{H}e) = \sqrt{\mathrm{E}Y^2 - \mathrm{E}(\hat{E}n^2)}. \tag{4.20}$$

By the expressions (4.5) and (4.9), we get

$$\mathrm{E}(\hat{H}e) = \left(He^2 + En^2 - \sqrt{\frac{r}{n}\mathrm{D}Y^2 + En^4}\right)^{1/2}.$$

In addition, we have

$$\mathrm{MSE}(\hat{H}e) = \mathrm{E}(\hat{H}e - He)^2 = \mathrm{E}(\hat{H}e^2) - 2He \cdot \mathrm{E}(\hat{H}e) + He^2,$$

where, $\hat{H}e^2 = \hat{\mathrm{E}}Y^2 - \hat{E}n^2$. Namely,

$$\mathrm{MSE}(\hat{H}e) = \mathrm{E}Y^2 - \mathrm{E}(\hat{E}n^2) - 2He \cdot \mathrm{E}(\hat{H}e) + He^2. \tag{4.21}$$

Finally, applying $\mathrm{E}Y^2$, $\mathrm{E}(\hat{E}n^2)$ and $\mathrm{E}(\hat{H}e)$ into the expression (4.21), the expression (4.19) can be got. □

From Theorems 5, 7, and 8, the following conclusions can be derived:

- Since $\mathrm{E}(\hat{E}x) = Ex$, $\lim_{n\to\infty} \mathrm{E}(\hat{E}n) = En$ and $\lim_{n\to\infty} \mathrm{E}(\hat{H}e) = He$, the estimator $\hat{E}x$ is the unbiased estimator, and the estimators $\hat{E}n$ and He are the asymptotic unbiased estimators of En and He, respectively.
- Since $\lim_{n\to\infty} \mathrm{MSE}(\hat{E}x) = 0$, $\lim_{n\to\infty} \mathrm{MSE}(\hat{E}n) = 0$ and $\lim_{n\to\infty} \mathrm{MSE}(\hat{H}e) = 0$, the MSE of the estimators $\hat{E}x$, $\hat{E}n$ and He converge to 0, respectively.
- Since $\lim_{n\to\infty} \mathrm{D}(\hat{E}x) = \lim_{n\to\infty} \mathrm{MSE}(\hat{E}x) = 0$, $\lim_{n\to\infty} \mathrm{D}(\hat{E}n) = \lim_{n\to\infty} \mathrm{MSE}(\hat{E}n) - (\mathrm{E}(\hat{E}n) - En)^2 = 0$ and $\lim_{n\to\infty} \mathrm{D}(\hat{H}e) = \lim_{n\to\infty} \mathrm{MSE}(\hat{H}e) - (\mathrm{E}(\hat{H}e) - He)^2 = 0$, $\hat{E}x$, $\hat{E}n$ and $\hat{H}e$ are all the consistent estimators.

5 Experiments

Generally, a concept's intension can be mapped into many extension sets with stable distribution. Thus, in order to obtain the stable intension of a concept, we give out the numerical characteristics (Ex, En, He) representing a concept's intension in advance, and then use the FGCT algorithm to generate the test sample. Finally, using the SBGCT-1stM, SBGCT-4thM, and MBGCT-SD algorithms to obtain the estimates representing the concept's intension so as to compare the stability of them. Applications of MBGCT-SD in image segmentation are also done to evaluate its validity and performance. The experiment hardware environment adopts a computer with Intel(R) Core(TM)2 Quad CPUT Q8300 @2.5 GHz and 2G memory.

5.1 Comparison of three BGCT algorithms

Based on the analysis for SBGCT-1stM and SBGCT-4thM, we give out Ex, En, and He values according to the proportion He/En: (*i*) $3He \leq En$; (*ii*) $3He > En$. In MBGCT-SD, the estimates $\hat{E}n$ and $\hat{H}e$ are related with m, so we use an iterative method to find the satisfactory solution m and the estimates $\hat{E}n$ and $\hat{H}e$. The specific steps are displayed in Algorithm 5.

Algorithm 5 The iterative process of m value and the estimates $(\hat{E}n, \hat{H}e)$ in MBGCT-SD

Input: The random sample $Sample = \{X_1, X_2, \cdots, X_n\}$, the sample size n and the initial value $m = 2$.

Output: The estimates $(\hat{E}n, \hat{H}e)$ and the satisfied solution m.

```
Begin m = 2;
[initial_En, initial_He]=MBGCT-SD(Sample, n, m);
while(1) do
   m = m+1;
   if (mod(n, m)== 0)
      [Ên, Ĥe]=MBGCT-SD(Sample, n, m);
   end if
   temp;
   if (abs(Ên-En)≤temp && abs(Ĥe-He)≤temp)
            /*En, He can be replaced by initial_En and initial_He respectively if
the true values En, He are unknown*/
      output(m, Ên, Ĥe);
      break;
   else if
      initial_En = Ên; initial_He = Ĥe;
   end if
end while
End
```

5.1.1 The sample size n is fixed

Calculate the estimates $\hat{E}x$, $\hat{E}n$, and $\hat{H}e$, their mean and average absolute errors (AAE, where, $\mathrm{AAE}(\hat{\theta}) = \frac{1}{T}\sum_{i=1}^{T}|\theta - \hat{\theta}_i|$), and their MSE ($T = 50$ times), where we set $n = 5000$.

(i) $3He \le En$

Let $(Ex = 25, En = 3, He = 0.1)$ and determine the satisfactory solutions $m = 10$ based on Algorithm 5. The results are shown in Fig. 6.[4] The mean, AAE, and MSE of $\hat{E}x$, $\hat{E}n$, and $\hat{H}e$ are shown in Table 1.

The experiment results indicate that the estimate $\hat{H}e$ is an imaginary number sometimes in SBGCT-1stTM and SBGCT-4thM (see the right figure in Fig. 6). We

[4]Note: if the estimates $\hat{E}n$ and $\hat{H}e$ are imaginary numbers respectively, we set $\hat{E}n = -0.2$ and $\hat{H}e = -0.2$.

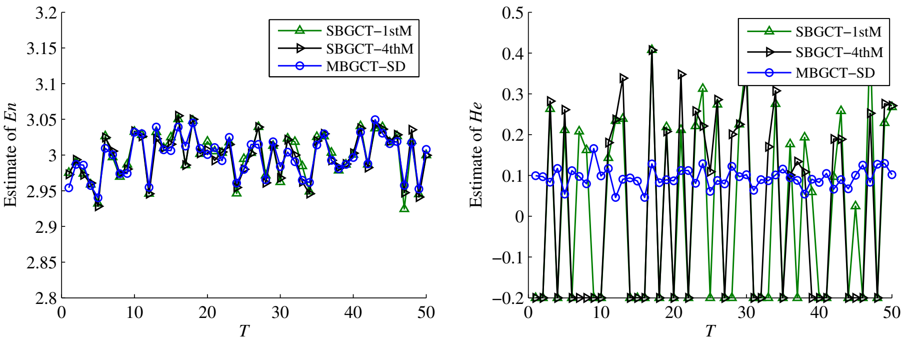

Fig. 6 The estimates $\hat{E}n$ and $\hat{H}e$ if $En = 3$, $He = 0.1$

can see that $\hat{H}e$ be an imaginary number has appeared 25 times in 50 experiments for SBGCT-1stM and SBGCT-4thM. The results are consistent with the theoretical analysis in Section 3.2. However, this situation does not appear in MBGCT-SD. In Table 1, the mean, AAE, and MSE of $\hat{H}e$ are received by excluding these imaginary numbers in SBGCT-1stM and SBGCT-4thM. From Table 1, AAE($\hat{H}e$) and MSE($\hat{H}e$) is larger in SBGCT-1stM and SBGCT-4thM than in MBGCT-SD, while the three BGCT algorithms can make a good estimate for En.

(*ii*) $3He > En$

Let ($Ex = 25$, $En = 1$, $He = 0.8$) and determine the satisfactory solutions $m = 1000$ based on Algorithm 5. The results are shown in Fig. 7. The mean, AAE, and MSE of $\hat{E}x$, $\hat{E}n$, and $\hat{H}e$ are shown in Table 2.

According to the analysis in Section 3.2, in SBGCT-1stM, $\hat{E}n$ will be larger than its true value En, simultaneously, $\hat{H}e$ will be less than the true value He when $3He > En$. The experiment results indicate that $\hat{E}n$ is larger than 1 and $\hat{H}e$ is less

Table 1 The mean, AAE, and MSE if $Ex = 25$, $En = 3$, $He = 0.1$

Estimate	Mean, AAE, MSE	SBGCT-1stM	SBGCT-4thM	MBGCT-SD
$\hat{E}x$	Mean ($\hat{E}x$)	25.0052	25.0052	25.0052
	AAE ($\hat{E}x$)	0.0357	0.0357	0.0357
	MSE ($\hat{E}x$)	0.0019	0.0019	0.0019
$\hat{E}n$	Mean ($\hat{E}n$)	2.9996	2.9982	2.9983
	AAE ($\hat{E}n$)	0.0258	0.0257	0.0231
	MSE($\hat{E}n$)	0.9849×10^{-3}	0.9674×10^{-3}	0.7652×10^{-3}
$\hat{H}e$	Mean ($\hat{H}e$)	0.2300	0.2363	0.0944
	AAE ($\hat{H}e$)	0.1396	0.1363	0.0186
	MSE ($\hat{H}e$)	0.0259	0.0247	0.6361×10^{-3}

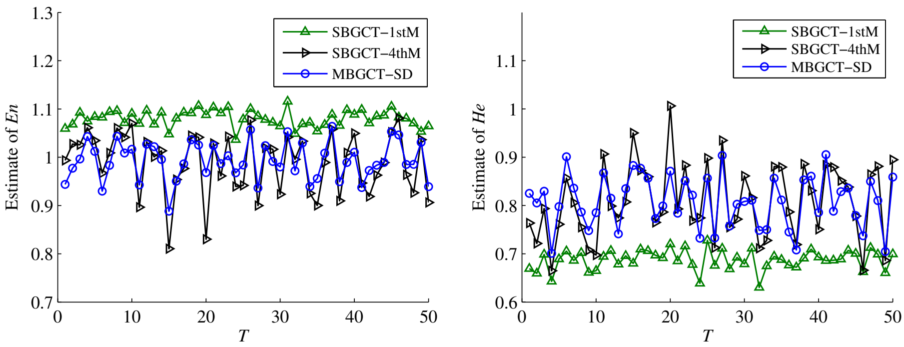

Fig. 7 The estimates $\hat{E}n$ and $\hat{H}e$ when $En = 1$, $He = 0.8$

than 0.8 (shown in Fig. 7). The SBGCT-4thM and MBGCT-SD have no large difference for $\hat{H}e$ and $\hat{E}n$, but the AAE($\hat{E}n$), MSE($\hat{E}n$), AAE($\hat{H}e$) and MSE($\hat{H}e$) are all smaller in MBGCT-SD from Table 2.

Overall, the above experimental results show that the MBGCT-SD is superior to other two BGCT algorithms, and it has better stability than others as well.

5.1.2 The sample size n is changing

Similar to the Section 5.1.1, comparing the mean and MSE of the estimates $\hat{E}n$ and $\hat{H}e$ with the increasing of sample sizes n (n is changing from 1000 to 20000 by step 1000) according to the above proportion He/En.

(i) $3He \leq En$

Let ($Ex = 25$, $En = 3$, $He = 0.1$). The estimated mean (Mean($\hat{E}n$), Mean($\hat{H}e$)) and MSE (MSE($\hat{E}n$), MSE($\hat{H}e$)) with the changing of sample size n are shown in Fig. 8.

Table 2 The mean and MSE if $Ex = 25$, $En = 1$, $He = 0.8$

Estimate	Mean, AAE, MSE	SBGCT-1stM	SBGCT-4thM	MBGCT-SD
$\hat{E}x$	Mean ($\hat{E}x$)	24.9997	24.9997	24.9997
	AAE ($\hat{E}x$)	0.0147	0.0147	0.0147
	MSE ($\hat{E}x$)	0.3160×10^{-3}	0.3160×10^{-3}	0.3160×10^{-3}
$\hat{E}n$	Mean ($\hat{E}n$)	1.0806	0.9887	0.9929
	AAE ($\hat{E}n$)	0.0806	0.0516	0.0327
	MSE ($\hat{E}n$)	0.0068	0.0041	0.0016
$\hat{H}e$	Mean ($\hat{H}e$)	0.6875	0.8084	0.8083
	AAE ($\hat{H}e$)	0.1125	0.0648	0.0449
	MSE ($\hat{H}e$)	0.0131	0.0060	0.0029

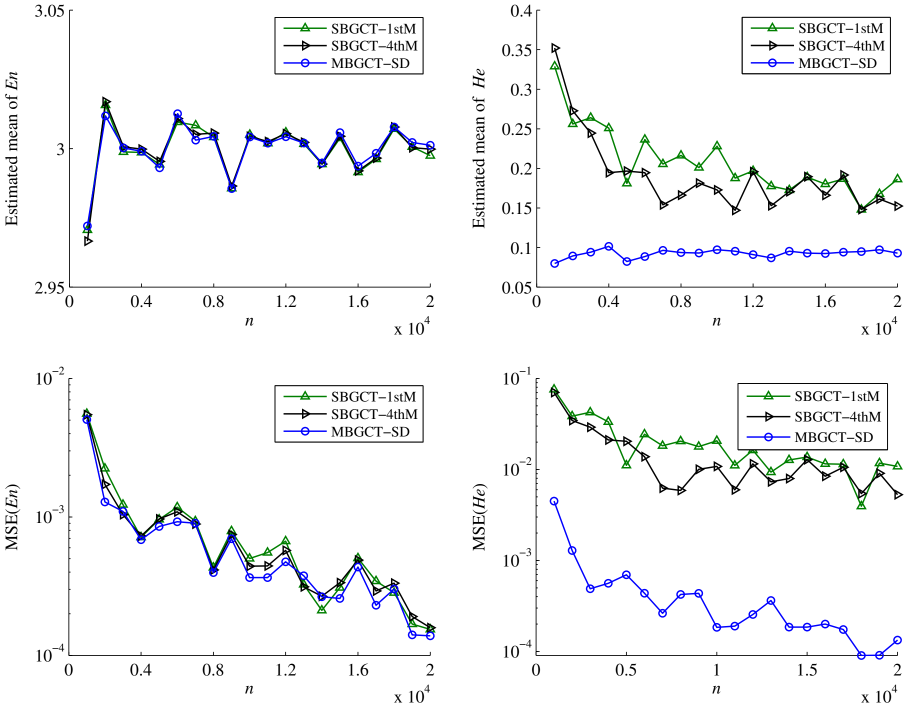

Fig. 8 The means and MSEs of $\hat{E}n$ and $\hat{H}e$ when $En = 3$, $He = 0.1$

Figure 8 shows that the estimated mean Mean($\hat{H}e$) in SBGCT-1stM and SBGCT-4thM is larger than the true value 0.1, but Mean($\hat{H}e$) is always close to the true value 0.1 in MBGCT-SD during the sample size n increasing from 1000 to 20,000 with the step 1000. Simultaneously, MSE($\hat{H}e$) approaches 0 faster in MBGCT-SD than in SBGCT-1stM and SBGCT-4thM. There is no significant differences about the estimated mean Mean($\hat{E}n$) and MSE($\hat{E}n$) in three BGCT algorithms with the increasing of sample size n.

(ii) $3He > En$

Let ($Ex = 25$, $En = 1$, $He = 0.8$). The estimated mean (Mean($\hat{E}n$), Mean($\hat{H}e$)) and MSE (MSE($\hat{E}n$), MSE($\hat{H}e$)) with the changing of sample size n are shown in Fig. 9.

Figure 9 shows that the estimate mean Mean($\hat{E}n$) is always larger than 1 and Mean($\hat{H}e$) is always smaller than 0.8 with the increasing of sample size n in the SBGCT-1stM, so MSE($\hat{E}n$) and MSE($\hat{H}e$) do not approach 0. In SBGCT-4thM and MBGCT-SD, there are no significant differences about the estimated Mean ($\hat{E}n$) and Mean ($\hat{H}e$), but MSE ($\hat{E}n$) and MSE ($\hat{H}e$) are smaller in MBGCT-SD than in SBGCT-4thM.

In summary, compared with the SBGCT-1stM and SBGCT-4thM, the advantages of MBGCT-SD are reflected in the following two aspects: (1) the MBGCT-SD always

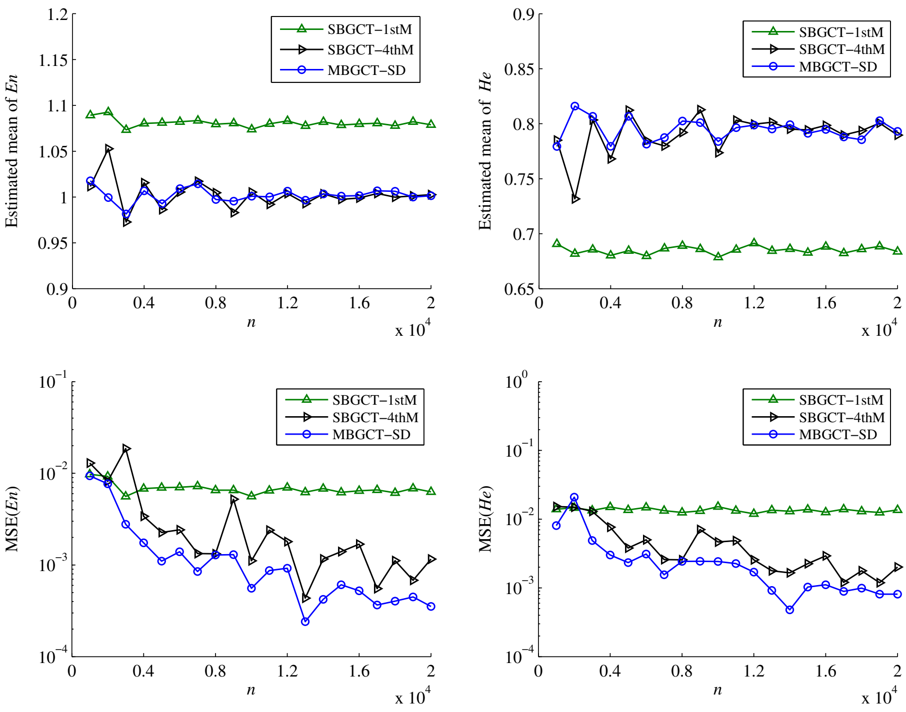

Fig. 9 The means and MSEs of $\hat{En}$ and $\hat{He}$ when $En = 1$, $He = 0.8$

gets better estimates than the other two BGCT algorithms whatever the ratio He/En is. It shows that the MBGCT-SD has stronger adaptability than the other two BGCT algorithms; (2) the experiment results indicate that the estimated Mean ($\hat{En}$) and Mean ($\hat{He}$) are closer to their true values, and MSE ($\hat{En}$) and MSE ($\hat{He}$) tend to zero faster than the other two BGCT algorithms when the sample size n is increasing, which shows that the MBGCT-SD has better convergence. Since the three BGCT algorithms make use of the same method to estimate the parameter Ex, that is, $\hat{Ex}$ is equal to the sample mean $\bar{X}$. Thus, there is no comparative analysis for Ex in the paper. The three BGCT algorithms have the same time complexity, i.e., $O(n)$.

5.2 Image segmentation based on MBGCT-SD

Image segmentation is an important issue of automatic image processing, and the basis of image analysis and understanding [50]. The basic task of image segmentation is to partition an image into non-overlapping regions according to the features of image so as to extract the object regions of interest [31]. The following two examples will illustrate the effectiveness of MBGCT-SD algorithm in image segmentation.

Example 2 Qin and Wu have applied the SBGCT-1stM and the SBGCT-4thM into the image segmentation, which are denoted as SBGCT-1stM-based method and

SBGCT-4thM-based method respectively. In the paper, the MBGCT-SD algorithm is applied to the image segmentation, and its validity and effectiveness are shown by comparing with some classical image segmentation methods, such as the Otsu method [27], the type-2 fuzzy set method [32], the SBGCT-1stM-based method [30], and the SBGCT-4thM-based method [41]. The segmentation results are shown in Figs. 10 and 11.

Figure 10 shows the segmentation results of comparing with the Otsu method, the type-2 fuzzy set method and the SBGCT-1stM-based method, wherein Fig. 10a represents the original images, and Fig. 10b represents the manually sketched images. Figure 11 shows the segmentation results of comparing with the Otsu method, the type-2 fuzzy set method, and the SBGCT-4thM-based method, wherein Fig. 11a represents the original images, which are named Block, Gearwheel, Potatoes, Fluocel, Rice, and Pcb from left to right, respectively, and Fig. 11b represents the manually sketched images.

In order to further assess the performance of the segmentation results, we consider the following index of misclassification error (ME) as empirical discrepancy criteria, proposed by Yasnoff et al. [45], which measures the disparity between the segmented and a reference image (manually sketched image) [2, 30, 41]. It should be mentioned that the reference image required for calculating the empirical discrepancy measure is obtained by manual segmentation. The misclassification error is given as

$$ME = 1 - \frac{|B_R \cap B_S| + |F_R \cap F_S|}{|B_R| + |F_R|}, \tag{5.1}$$

where B_R and F_R represent the background and foreground pixels of the reference image, respectively. B_S and F_S refer to corresponding pixels of the segmented image, while $|\cdot|$ denotes the cardinality of a set.

Figure 12 shows the ME values of our method and other methods. Figure 12a shows the ME values of our method and other methods, including the Otsu method, the type-2 fuzzy set method, and the SBGCT-1stM method, wherein Img1, Img2, and Img3 appeared in Fig. 12a refer to the first image, the second image, and the third image appeared in Fig. 10a, respectively. Figure 12b shows the ME values of our method and other methods, including the Otsu method, the type-2 fuzzy set method, and the SBGCT-4thM method. In Fig. 12a, b, "Mean" and "SD" represent the mean and standard deviation (SD) of the ME values respectively.

Figure 12a, b shows that the ME values of our method are generally lower for most images, and ME values' mean and SD are also smaller than other methods. The results validate the proposed method can segment objects in image effectively.

Example 3 The pulse coupled neural network (PCNN) is a novel neural network model to simulate the synchronous phenomenon in the visual cortex system of the mammals [13]. It has been widely applied into the field of image processing and pattern recognition [26, 40]. Wei proposed a new method based on the simplified model of PCNN (S-PCNN) to segment the images automatically [40]. We use MBGCT-SD to segment the images taken from the literature [40] and compare it with the

(a) Original images

(b) Manually sketched images

(c) Type-2 fuzzy set method

(d) Otsu method

(e) SBGCT-1stM-based method

(f) The proposed method

Fig. 10 Segmentation of different images by our method and other methods: Otsu, type-2 fuzzy set, and SBGCT-1stM-based, respectively

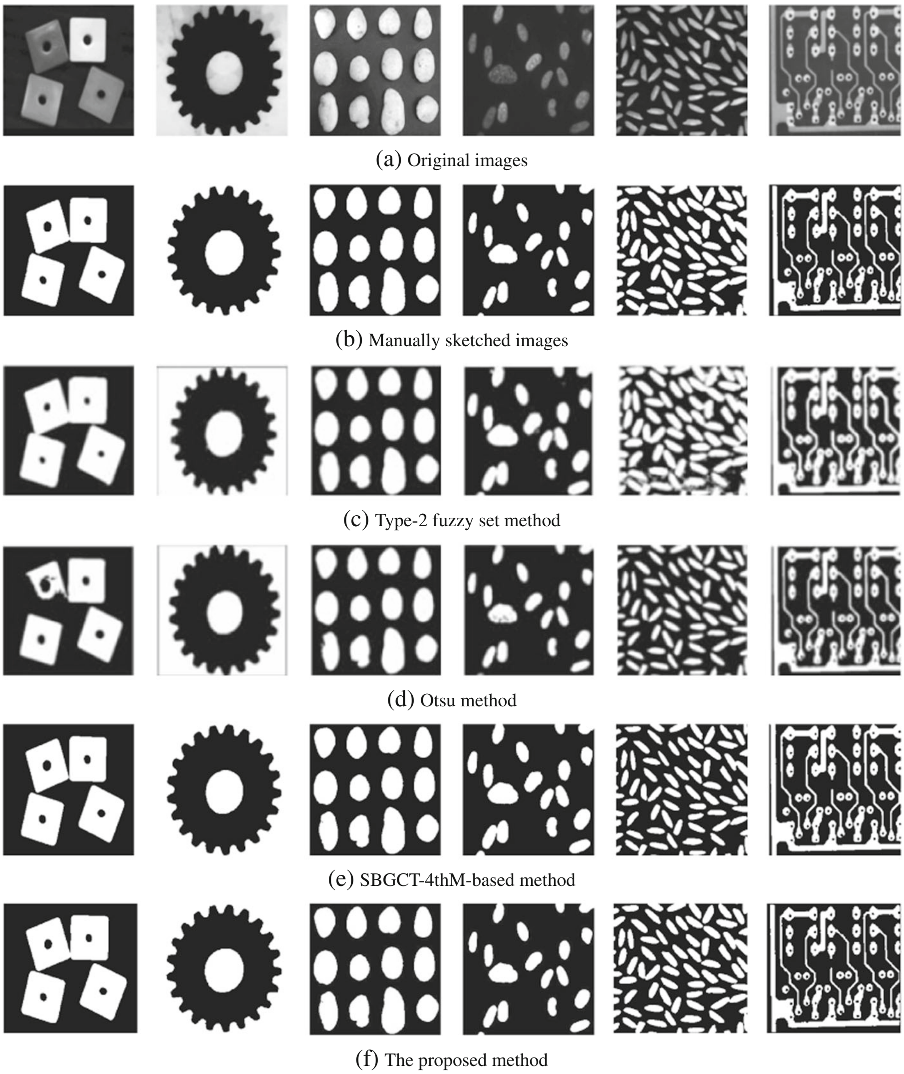

Fig. 11 Segmentation of different images by our method and other methods: Otsu, type-2 fuzzy set, and SBGCT-4thM-based, respectively

Otsu method [27], the GMM method [9], the K-means method [14], and the S-PCNN method [40]. The results are presented in Fig. 13, wherein the original images are shown in Fig. 13a, and the results of the Otsu method, the GMM method, the K-means method, and the proposed method are shown in Fig. 13b–f.

From Fig. 13, the proposed method can get better segmentation results than other methods. For example, for the first image of Fig. 13a, our method performs better segmentation for "face," "eyes," "hair," and "fingers," while other methods separate the

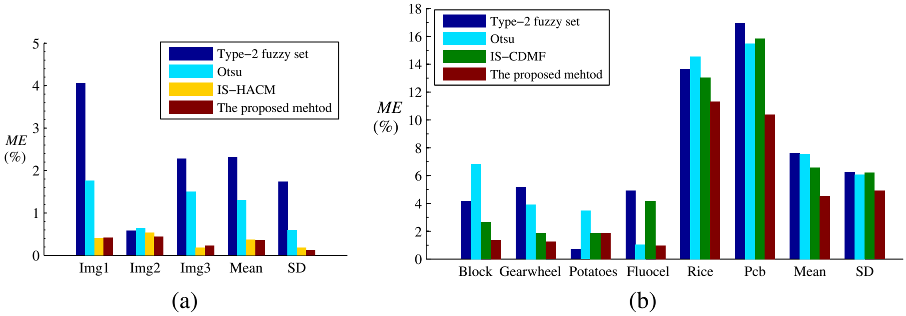

Fig. 12 ME values of our method and other methods: Otsu, type-2 fuzzy set, SBGCT-1stM-based, and SBGCT-4thM-based, respectively

image "girl" overly. For the second image of Fig. 13a, our method separates the blood cells from its background clearly and the number of cells based on our segmentation result can be counted easily, while the other methods are not. For the third image of Fig. 13a, every single cell is distinctly separated from each other in the segmentation result by our method, while some cells is difficult to be identified in other methods. This is mainly because our method has some advantages in expressing the uncertain information for the transition region between background and foreground, which reflects the superiority of Gaussian cloud model using three numerical characteristics (Ex, En, He) to express a uncertain concept.

Example 4 Cai proposed a two-stage segmentation method based on the Mumford-Shah model(T-SSMMSM) [54], where the first stage is to find a smooth solution g to convex variant of the Mumford-Shah model, and then in the second stage the segmentation is done by the obtained thresholding g. Li introduced a two-stage model for multi-channel image segmentation (T-SMMCIS) [55], where the first stage is to acquire a smooth solution u from convex variational model related to minimal surface property and different data fidelity terms, and then in the second stage the smoothed image u is segmented by thresholding. Now, we compare our method with the literatures [54, 55]. The results are presented in Figs. 14, 15, and 16.

Figure 14a, d gives the clean and the noisy images (Gaussian noise with zero mean and variance 0.03 [54]). The corresponding segmentation results of T-SSMMSM with four-phase noisy image are given in Fig. 14b, e. The proposed method results are shown in Fig.14c, f. In contrast, there is almost no difference between T-SSMMSM and our method for clean image and noisy image. Figure 15 shows the results of the T-SSMMSM with three-phase image [54] (Fig. 15b) and our method (Fig. 15c) for the given image (Fig. 15a). By contrast, our method gives the relatively clear boundaries than the T-SSMMSM for the original image. Figure 16 shows the results of the T-SMMCIS with two-phase segmentation [55] (Fig. 16b, c) and our method (Fig. 16d) for the given image (Fig. 16a). Comparatively, our method also gets better segmentation result than the T-SMMCIS with two-phase segmentation. In above segmentation results, we consider the situation of segmenting the gray image into parts: foreground

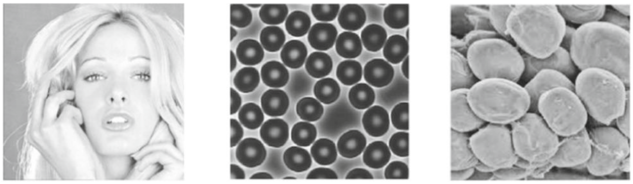

(a) Original images

(b) Otsu method

(c) GMM method

(d) K-means method

(e) S-PCNN method

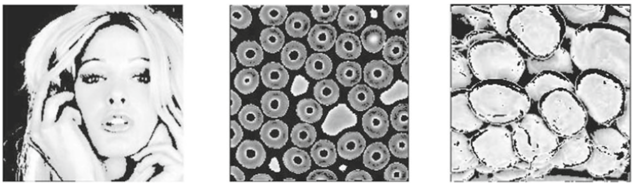

(f) The proposed method

Fig. 13 Segmentation of different images by our method and other methods: Otsu, GMM, K-means, and S-PCNN, respectively

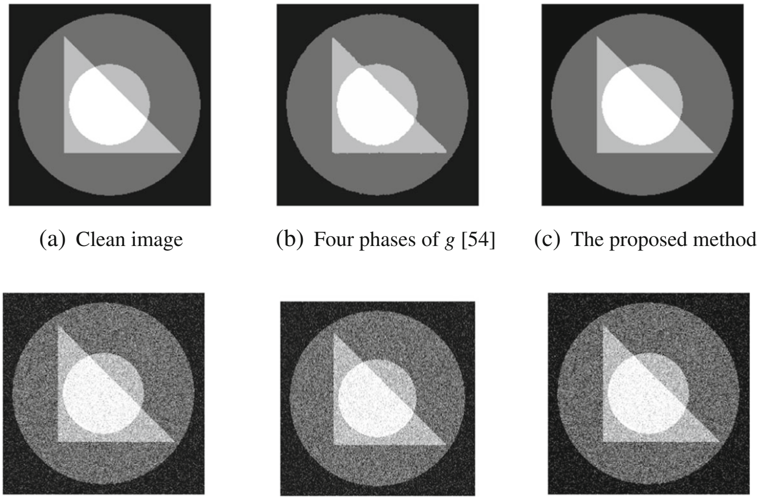

(a) Clean image (b) Four phases of g [54] (c) The proposed method

(d) Given noisy image (e) Fourth phase [54] (f) The proposed method

Fig. 14 Segmentation of different images by our method and T-SSMMSM with four-phase noisy image [54]

(a) Given image (b) Three phases from g [54] (c)The proposed method

Fig. 15 Segmentation of different images by our method and T-SSMMSM with three-phase image [54]

(a) Given image (b) T-SMMCIS [55] ($\|u-f\|_2^2$) (c) T-SMMCIS [55] ($\|u-f\|_1$) (d) The proposed method

Fig. 16 Segmentation of different images by our method and T-SMMCIS with two-phase segmentation [55] (object) and background regions. The proposed method can get better segmentation results.

6 Conclusions and prospects

In this paper, the backward Gaussian cloud transformation (BGCT) algorithm is studied. The limitations of two existing BGCT algorithms proposed in literatures [20, 37] are analyzed in detail respectively, and a novel BGCT algorithm (MBGCT-SD) is proposed. The convergence of MBGCT-SD is analyzed in detail. Several comparative experiments and its applications to image segmentation are given. Experimental results presented here have demonstrated that the MBGCT-SD algorithm is able to obtain better estimates for entropy En and hyper entropy He whatever the ratio He/En is, while other two methods are not. Meanwhile, we compare the T-SSMMSM [54], the T-SMMCIS with two-phase segmentation [55], and the proposed method through the gray image segmentation. The segmentation results show the performance of the proposed method.

It is easy to know the uncertain concept for human thinking, and the mutual transformation between the intension and the extension of a concept can be conducted automatically in human brain. Forward cloud transformation and backward cloud transformation in cloud model provide a way to realize the transformation between intension and extension of a concept through computer algorithm. Therefore, a interesting aspect worthy of investigation is to research the bidirectional cognitive process based on cloud transformation and human cognition in the future work.

Acknowledgments The authors would like to thank for a grant from the National Natural Science Foundation of China (61272060, 61562001, 11601012), the Key Natural Science Foundation of Chongqing (CSTC2013jjB40003), the Research Project of Beifang University of Nationalities (2016SXKY05), and the Science and Technology Research Project of Ningxia Higher Educational Institution (NGY2016143).

References

1. Angiulli, F., Fassetti, F.: Indexing uncertain data in general metric spaces. IEEE Trans. Knowl. Data Eng. **24**(9), 1640–1657 (2012)
2. Arifin, A.Z., Asano, A.: Image segmentation by histogram thresholding using hierarchical cluster analysis. Pattern Recogn. Lett. **27**(13), 1515–1521 (2006)
3. Cai, W.: The extension set and non-compatible problems. Journal of Science Explore (in Chinese) **1**, 83–97 (1983)
4. Casella, G., Berger, R.L.: Statistical Inference. China Machine Press, Beijing (2002)
5. Deng, J.: Grey Systems. China Machine Press, Beijing (1988)
6. Deng, W., Wang, G., Zhang, X.: A novel hybrid water quality time series prediction method based on cloud model and fuzzy forecasting. Chemom. Intell. Lab. Syst. **149**, 39–49 (2015)
7. Ding, W., Guan, Z., Shi, Q., Wang, J.: A more efficient attribute self-adaptive co-evolutionary reduction algorithm by combining quantum elitist frogs and cloud model operators. Inform. Sci. **293**, 214–234 (2015)
8. Embrechts, P., Klüppelberg, C., Mikosch, T.: Modelling Extremal Events for Insurance and Finance. Springer, Berlin (2002)

9. Fan, S., Lin, Y., Wu, C.: Image thresholding using a novel estimation method in generalized gaussian distribution mixture modeling. Neurocomputing **72**(1-3), 500–512 (2008)
10. Hirota, K.: Concetps of probabilistic sets. Fuzzy Set. Syst. **5**(1), 31–46 (1981)
11. Hu, Q., Yu, D., Pedrycz, W., Chen, D.: Kernelized fuzzy rough sets and their applications. IEEE Trans. Knowl. Data Eng. **23**(11), 1649–1667 (2011)
12. Jiang, B., Pei, J., Tao, Y., Lin, X.: Clustering uncertain data based on probability distribution similarity. IEEE Trans. Knowl. Data Eng. **25**(4), 751–763 (2013)
13. Johnson, J.L., Padgett, M.L.: Pcnn models and applications. IEEE Trans. Neural Netw. **10**(3), 480–498 (1999)
14. Kanungo, T., Mount, D., Netanyahu, N., Piatko, C., Silverman, R., Wu, A.: An efficient k-means clustering algorithm: analysis and implementation. IEEE Trans. Pattern Anal. Mach. Intell. **24**(7), 881–892 (2002)
15. Li, D.: The cloud control method and balancing patterns of triple link inverted pendulum systems. Eng. Sci. **1**(2), 41–46 (1999)
16. Li, D., Du, Y.: Artificial Intelligence with Uncertainty. Chapman and Hall/CRC, London (2007)
17. Li, D., Liu, C.: Study on the universality of the normal cloud model. Eng. Sci. **6**(8), 28–34 (2004)
18. Li, D., Liu, C., Gan, W.: A new cognitive model: cloud model. Int. J. Intell. Syst. **24**(3), 357–375 (2009)
19. Liu, B., Xiao, Y., Yu, P., Cao, L.: Uncertain one-class learning and concept summarization learning on uncertain data streams. IEEE Trans. Knowl. Data Eng. **26**(2), 468–484 (2014)
20. Liu, C., Feng, M., Dai, X., Li, D.: A new algorithm of backward cloud. Journal of System Simulation **16**(11), 2417–2420 (2004)
21. Liu, C., Li, D., Du, Y., Han, X.: Some statistical analysis of the normal cloud model. Inf. Control. **34**(2), 236–248 (2005)
22. Liu, X., Pedrycz, W., Song, M.: The development of fuzzy rough sets with the use of structures and algebras of axiomatic fuzzy sets. IEEE Trans. Knowl. Data Eng. **23**(3), 443–462 (2009)
23. Liu, Y., Li, D., He, W., Wang, G.: Granular computing based on gaussian cloud transformation. Fundamenta Informaticae **127**(1-4), 385–398 (2013)
24. Lu, H., Wang, Y., Li, D., Liu, C.: The application of backward cloud in qualitative evaluation. Chinese Journal of Computers **26**(8), 1009–1014 (2003)
25. Moore, R.E.: Interval Analysis, pp. 25–29. Prentice-Hall, Englewood Cliffs, NJ (1996)
26. Muresan, R.C.: Pattern recognition using pulse-coupled neural networks and discrete fourier transforms. Neurocomputing **51**, 487–493 (2003)
27. Otsu, N.: A threshold selection method from gray-level histograms. IEEE Trans. Syst. Man Cybern. SMC **9**(1), 62–66 (1979)
28. Pawlak, Z.: Rough sets. Int. J. Comput. Inform. Sci. **11**(5), 341–356 (1982)
29. Pawlak, Z., Skowron, A.: Rough sets: some extension. Inform. Sci. **177**(1), 28–40 (2007)
30. Qin, K., Xu, K., Liu, F., Li, D.: Image segmentation based on histogram analysis utilizing the cloud model. Comput. Math. Appl. **62**, 2824–2833 (2011)
31. Snyder, W.E., Qi, H.: Machine Vision. Cambridge University Press, Cambridge (2004)
32. Tizhoosh, H.: Image thresholding using type ii fuzzy sets. Pattern Recogn. **38**(12), 2363–2372 (2005)
33. Wallerstein, I.: The Uncertainties of Knowledge. Temple University Press, Philadelphia (2004)
34. Wang, G.: Rough set based uncertainty knowledge expressing and processing. In: 13th International Conference of Rough Sets, Fuzzy Sets, Data Mining and Granular Computing, pp. 11–18. Springer, Berlin Heidelberg, Moscow, Russia (2011)
35. Wang, G., Xu, C.: Cloud model—a bidirectional cognition model between concept's extension and intension. In: First International Conference on Advanced Machine Learning Technologies and Applications, pp. 391–400. Springer, Berlin Heidelberg, Cairo, Egypt (2012)
36. Wang, G., Xu, C., Zhang, Q., Wang, X.: A multi-step backward cloud generator algorithm. In: The 8th International Conference on Rough Sets and Current Trends in Computing, pp. 313–322. Springer, Berlin Heidelberg, Chengdu, China (2012)
37. Wang, L.: The basic mathematical properties of normal cloud and cloud filter. Personal Communication (2011)
38. Wang, S., Li, D., Shi, W., Li, D., Wang, X.: Cloud model-based spatial data mining. Geographical Information Science **9**(1–2), 60–70 (2003)

39. Wang, Z.: Probability Theory and its Applications. Beijing Normal University Press, Beijing (1995)
40. Wei, S., Hong, Q., Hou, M.: Automatic image segmentation based on pcnn with adaptive threshold time constant. Neurocomputing **74**(9), 1485–1491 (2011)
41. Wu, T., Qin, K.: Image segmentation using cloud model and data field. Pattern Recogition and Artificial Intelligence **25**(3), 397–405 (2012)
42. Wu, W., Chen, K., Zeng, B., Yang, M., Geng, S.: Cloud-based decision framework for waste-to-energy plant site selection—a case study from China. Waste Manag. **48**, 593–603 (2016)
43. Wu, Z., Jia, W., Zhao, L., Wu, C.: Maximum wind power tracking based on cloud rbf neural network. Renew. Energy **86**, 466–472 (2016)
44. Xu, J.: Normal cloud heavy-tailed model research based on the semi-invariantion. Journal of Software Engineering **9**(2), 276–286 (2015)
45. Yasnoff, W.A., Mui, J.K., Bacus, J.W.: Error measures for scene segmentation. Pattern Recogn. **9**(4), 217–231 (1977)
46. Zadeh, L.: Fuzzy sets. Inf. Control. **8**(3), 338–353 (1965)
47. Zadeh, L.: Towards a theory of fuzzy information granulation and its centrality in human reasoning and fuzzy logic. Fuzzy Set. Syst. **90**(2), 111–127 (1997)
48. Zhang, Q., Wang, G.: The uncertainty measure of hierarchical quotient space structure. Math. Probl. Eng. **2011**, 1–16 (2011)
49. Zhang, W., Liu, S., Sun, B., Liu, Y., Pecht, M.: A cloud model-based method for the analysis of accelerated life test data. Microelectron. Reliab. **55**, 123–128 (2015)
50. Zhang, Y.: Image Engineering, 2nd edn. Tsinghua University Press, Beijing (2007)
51. Zhang, Y., Zhang, W., Lin, Q., Lin, X.: Effectively indexing the multidimensional uncertain objects. IEEE Trans. Knowl. Data Eng. **26**(3), 608–622 (2014)
52. Zhao, K.: Set Pair Analysis and its Primary Application. Zhejiang Science and Technology Press, Hangzhou (2000)
53. Zhou, Q., Wang, W., Pang, Y., Zhou, Z., Luo, H.: Temporal and spatial distribution characteristics of water resources in Guangdong Province based on a cloud model. Water Science and Engineering **8**(4), 263–272 (2015)
54. Cai, X., Chan, R., Zeng, T.: A two-stage image segmentation method using a convex variant of the Mumford-Shah model and thresholding. SIAM J. Imag. Sci. **6**(1), 368–390 (2013)
55. Li, Z., Zeng, T.: A two-stage image segmentation model for multi-channel images. Communications in Computational Physics **19**(4), 904–926 (2016)